Solid-Liquid Equilibrium of *Tröger*'s Base Enantiomers in Ethanol: Experiments and Modelling

by **Jörg Worlitschek**[a]), **Marcello Bosco**[a]), **Markus Huber**[a]), **Volker Gramlich**[b]), and **Marco Mazzotti***[a])

[a]) Institute of Process Engineering, ETH Swiss Federal Institute of Technology Zürich, Sonneggstrasse 3, CH-8092 Zürich (tel.: ++41-1-632-2456; fax: ++41-1-632-1141; e-mail: mazzotti@ivuk.mavt.ethz.ch)
[b]) Laboratory for Crystallography, ETH Swiss Federal Institute of Technology Zürich, Sonneggstrasse 5, CH-8092 Zürich

Thermodynamic properties of the enantiomers of the *Tröger*'s base as crystals and in ethanol solutions have been studied by means of a suite of analytical techniques. We report the melting diagrams of the two enantiomers, providing evidence for the formation of a solid racemic compound. We present also ternary equilibrium data about the solubility of the two enantiomers in ethanol at 25°, 35°, and 50°. The melting-diagram data are described well by the *Schroeder–Van Laar* and *Prigogine–Vieland* equations, when the melting temperatures and enthalpies of pure enantiomer and of the racemic compound are provided and with the assumption that the melting behavior is ideal. The ternary equilibrium data were well-described when nonideality of mixtures of ethanol and the enantiomers is accounted for in terms of the non-random two liquids (NRTL) model. Finally, we present the newly determined X-ray crystal structure of an orthorhombic form of the pure *Tröger*'s base (+)-enantiomer.

1. Introduction. – The need to produce enantiomerically pure substances cannot always be fulfilled through enantioselective chemical or enzymatic catalysis. Therefore, the development of separation processes to resolve racemic mixtures into pure enantiomers has gained more and more importance over the last years. Crystallization and chromatography are key operations in this context [1–7], the latter in particular being applied in the continuous operating mode offered by the 'simulated-moving-bed' technology [8]. A combination of chromatography, used for initial enrichment of the racemic mixture, followed by crystallization, for the final purification of the enantiomers, has also been proposed [7][9]. A thorough knowledge of the system thermodynamics, *i.e.*, the solid-liquid ternary equilibrium among the two enantiomers and the solvent of choice, is the basis for the design of the enantioselective-crystallization step [10]. An overview of different types of binary mixtures of enantiomers and of their properties in solution can be found in a seminal book [3]. More recently, data about the enantiomers of praziquantel in MeOH [11], those of mandelic acid in water [12], and the enantiomers of propranolol hydrochloride in a mixed MeOH/acetone solvent have been reported [13].

In this paper, we study the ternary solid-liquid equilibrium in EtOH of the enantiomers of (5*R*,11*R*)-2,8-dimethyl-6*H*,12*H*-5,11-methanodibenzo[*b*,*f*][1,5]diazocine, generally known as *Tröger*'s base. The molecule is chiral with a C_2 axis of symmetry due to the blocked conformation of the two N-atoms of the methanodiazocine bridge. As such, it is frequently used as a model system in various fields, including chiral chromatography [14–17], and its derivatives have been used for a suite

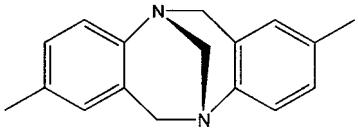

Tröger's base

of applications in organic chemistry and biochemistry [18][19]. The study of this system is interesting *per se*, as well as in view of the design of an integrated chromatography-crystallization process for its enantioseparation.

We present and discuss experimental methods and results concerning binary (enantiomer–enantiomer) and ternary (enantiomer–enantiomer–solvent) systems, as well as the solid-phase properties of *Troger*'s base. Then, binary and ternary solid-liquid equilibria are described by means of a proper solution model to calculate the activity coefficients, when necessary. Finally, the model results and the experimental data are compared and discussed.

2. Experimental. – 2.1. *Materials.* EtOH, purity ≥99.9%, was obtained from *J. T. Baker*, NL-Deventer. (+)-*Tröger*'s base, (+)-(5*R*,11*R*)-2,8-dimethyl-6*H*,12*H*-5,11-methanodibenzo[*b*,*f*][1,5]diazocine, and (−)-*Tröger*'s base, (−)-(5*R*,11*R*)-2,8-dimethyl-6*H*,12*H*-5,11-methanodibenzo[*b*,*f*][1,5]diazocine, chemical formula $C_{17}H_{18}N_2$, $M = 250.35$ g/mol, purity ≥99%, were from *Fluka AG*, CH-Buchs. Racemic (±)-*Tröger*'s base, purity 98%, was delivered by *Aldrich AG*, CH-Buchs and was purified before use by recrystallizing twice from EtOH.

2.2. *Methods. DSC Measurements:* DSC Measurements were carried out with a *Mettler DSC 822e* calorimeter (*Mettler-Toledo GmbH*, Schwerzenbach, Switzerland). Melting points and melting enthalpies of the pure enantiomers and of the racemic compound as well as melting temperatures of mixtures of different compositions of (+)- and (−)-*Tröger*'s base- (−) were determined. Mixtures were prepared by weighing certain amounts of (−)-*Tröger*'s base and the racemic compound and grinding the mixtures for 15 min in a mortar. DSC Aluminium pans were filled with samples of *ca.* 5 mg, and the pans were covered with perforated tops. N_2 was used for purging. The samples were heated from 20° to 140° at a rate of 3°/min. This heating rate was verified to have negligible effect on DSC results in the investigated range of 0.5°/min to 10°/min.

Binary and Ternary Equilibrium Measurements: Phase-equilibrium conditions were established wtih a *GFL 1086* waterbath shaker (±0.1°; GFL GmbH, Burgwedel, Germany). Samples of binary and ternary mixtures of *Tröger*'s base enantiomers and EtOH in 4.5 ml flasks were treated with ultrasound for 5 min and shaken at 150 rpm and constant temp. for at least 2 h to establish equilibrium conditions. The liq. phase was decanted and filtered through 0.2 μm membrane filters. The filtrate was weighed, diluted with a known mass of EtOH, and analyzed by HPLC thrice. HPLC Analyses were performed on a *Waters 2690 Separation Module* (*Waters*, Milford MA, USA) with a *Waters 996* photodiode-array detector (287 nm) on a *Chiracel OJ* chiral column (0.46 cm × 25 cm; *Diacel Chemical Industries*, Osaka, Japan), EtOH/hexane 50:50. To cross-check the HPLC results, some filtrate samples were subjected to thermogravimetric analysis (TGA) on a *Mettler TGA/SDTA 851e* thermobalance (*Mettler-Toledo GmbH*, Schwerzenbach, Switzerland). It is worth noting that the sampling, filtration, and dilution steps were performed in a temperature-controlled room at a temp. equal to the equilibrium temp. so as to avoid any perturbation of the thermodynamic equilibrium during the handling of the samples. The crystals obtained were washed with small amounts of EtOH and either diluted for further HPLC analysis, or directly analyzed by TGA, or dried and analyzed by X-ray diffraction (XRD). X-Ray analysis was performed with a *Picker-Stoe* single-crystal diffractometer (*Stoe & Cie GmbH*, Darmstadt, D).

3. Experimental Results. – For the sake of clarity in the interpretation of the results, we present here some information about the behavior of the *Tröger*'s base/EtOH system. *Tröger*'s base is present as both enantiopure crystals and racemic compound, and exhibits the eutectic behavior typical in solid-liquid equilibria. Thus, the binary

solid-liquid-equilibrium diagram for the Tröger's base enantiomers is qualitatively similar to the one illustrated in *Fig. 1, a*. Moreover, the ternary solid-liquid equilibria, including also the solvent, can be illustrated at a given temperature in a ternary diagram, as shown in *Fig. 1, b*. No evidence for the formation of solvates (ethanolates) has been observed in our experiments.

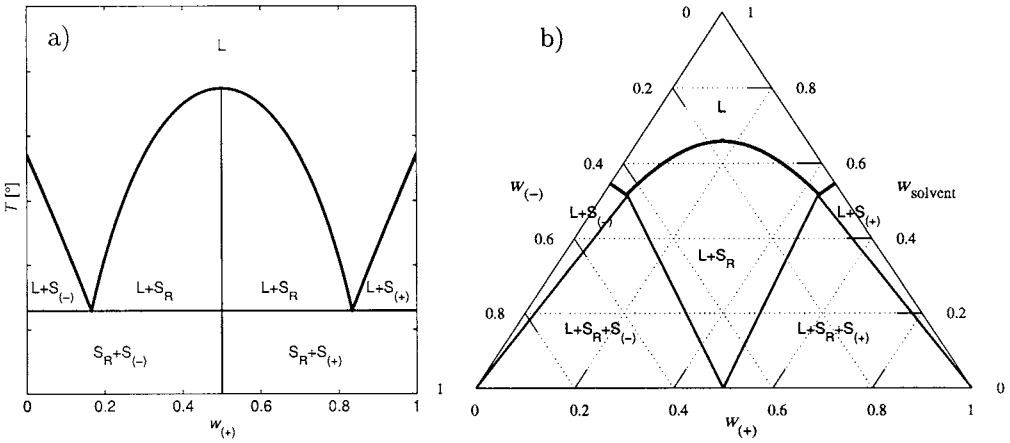

Fig. 1. *Examples of* a) *a phase diagram of a binary system with two enantiomers that form a racemic compound and* b) *an isothermal ternary phase diagram of a system including a solvent and two enantiomers that form a racemic compound*. Liquid phases are indicated with 'L', while racemic and enantiopure solid phases are indicated with 'S_R', 'S_-', and '$S_{(+)}$', respectively.

3.1. *Binary Solid-Liquid Equilibrium*. Experimental data for the binary solid-liquid equilibrium for the *Tröger*'s base enantiomers are reported in *Tables 1* and *2*. A few characteristic DSC heat-flux scans are shown in *Fig. 2*, and the melting diagram is plotted in *Fig. 3*. The data are based on DSC measurements of mixtures of the *Tröger*'s base enantiomers in the mass-fraction range $0 \leq w_{(+)} \leq 0.5$ (for symmetry). Only one peak is observed for the pure (−)-enantiomer ($w_{(+)} = 0$, first scan in *Fig. 2*), for the racemic mixture ($w_{(+)} = 0.5$, second scan in *Fig. 2*), and for a mixture very close to the eutectic condition ($w_{(+)} = 0.153$, fourth scan in *Fig. 2*). The melting temperatures (T_m) of pure *Tröger*'s base (−)- and of the racemic compound (both determined as the onset temperatures of the endothermic peak) are 129.79° and 135.71°, respectively, and are plotted as solid triangles in *Fig. 3*. The corresponding heats of fusion ($\Delta_{fus}H$) are 80.08 *J*/g for the pure enantiomer and 99.70 *J*/g for the solid racemic compound. Melting temperatures and the heats of fusion of the enantiopure and racemic

Table 1. *Enthalpy of Fusion* Δ_{fus}H [J/g] *and Melting Temperature* T_m [°] *of Enantiopure (+)*-Tröger's *Base and (±)*-Tröger'*s Base Racemate*. Mean values and 95%-confidence intervals based on DSC measurements of three samples.

	$\Delta_{fus}H$ [J/g]	T_m [°]
(+)-*Tröger*'s base	80 ± 2	129.8 ± 0.2
Racemate	100 ± 2	135.7 ± 0.3

Table 2. *DSC Data from Mixtures of* Tröger's *Base Enantiomers* (see DSC scans in *Fig. 2*)

$w_{(+)}$[a])	T_1 [°][b])	T_2 [°][c])
0.045	118.2	126.4
0.09	119.3	123.1
0.15	119.1	119.7
0.229	119.7	125.6
0.286	119.3	130.2
0.341	119.0	132.8
0.421	119.6	136.0

[a]) Mass fraction. [b]) Onset temperature of the first peak. [c]) Peak temperature of second peak.

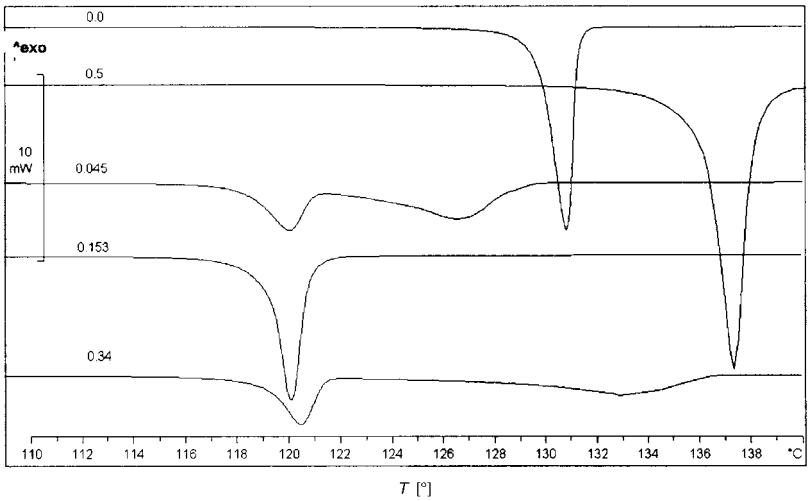

Fig. 2. *DSC Scans of five different samples of binary mixtures of (+)- and (−)-*Tröger's *base with given mass fractions* $w_{(+)}$ *in the temperature range 110°–140°*. From top to bottom: enantiopure (−)-*Tröger*'s base, racemic compound ($w_{(+)}=0.5$), a mixture with $w_{(+)}=0.045$, a mixture exhibiting a melting temperature corresponding to the eutectic point ($w_{(+)}=0.153$), and a mixture with $w_{(+)}=0.34$.

compounds are reported also in *Table 1*. The DSC measurements of mixtures of *Tröger*'s base enantiomers in the range $0<w_{(+)}<0.5$, with $w_{(+)}$ different from those of the eutectic mixture, lead to two endothermic peaks, as shown in the third and fifth DSC scans of *Fig. 2*, where $w_{(+)}=0.045$ and $w_{(+)}=0.34$, respectively. Here, the onset temperature of the first peak at lower temperature corresponds to the *solidus* line, *i.e.*, the eutectic (see boxes in *Fig. 3* and data presented in *Table 2*), and the peak temperature of the second peak at higher temperature corresponds to the *liquidus* line (see circles in *Fig. 3*). In summary, the results of the binary solid-liquid equilibrium of the *Tröger*'s base enantiomers indicate the presence of a racemic compound that leads to a eutectic point of *ca.* 119°, and a composition of $w_{(+)}\approx 0.15$. For symmetry, a eutectic point with the same melting temperature occurs at $w_{(-)}\approx 0.15$.

3.2. *Ternary Solid-Liquid Equilibrium.* The experimental results for the ternary solid-liquid equilibria of the *Tröger*'s base enantiomers and EtOH at 25°, 35°, and 50°

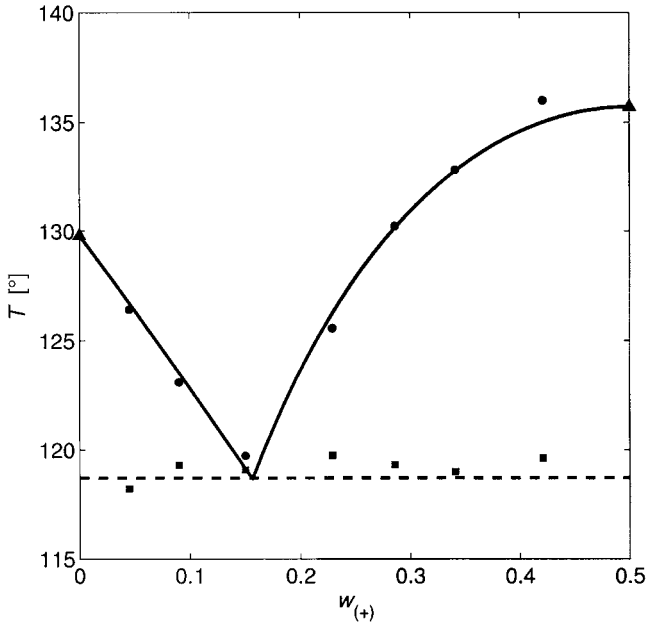

Fig. 3. *Melting-point diagram of* Tröger's *base enantiomer mixtures, as determined from DSC data.* Onset temperature of heat-flux peak (melting temperatures) of enantiopure and racemic compound (triangles); onset temperature of first peak corresponding to the eutectic point (squares); peak temperature of the second peak (circles); calculated binary (*liquidus*) equilibrium (solid line) based on *Eqns. 1* and *2*; calculated eutectic (*solidus*) temperature (dashed line).

are reported in *Table 3* and illustrated in *Fig. 4*. The composition of the solution in equilibrium with a solid precipitate is reported in *Table 3*; here the 95% confidence limits for the experimentally measured values of the enantiomer mass fractions are also indicated, whereas the EtOH mass fraction is calculated. The same data are plotted in the standard ternary diagram of *Fig. 4*.

For each series of isothermal data, three experimental points are to be highlighted. The first point of each series has been obtained by starting from the solid racemic compound and, in fact, exhibits within the experimental error the same concentration for the two enantiomers. This provides the solubility of the solid racemic compound at each temperature; these values are 27.6 g/kg of solution at 25°, 40.6 g/kg at 35°, and 71.8 g/kg at 50°. The last point of each series has been obtained with the pure (−)-enantiomer, hence it provides its solubility, *i.e.*, 51.8 g/kg of solution at 25°, 79.0 g/kg at 35°, and 118.5 g/kg at 50°. Finally, the point in each series that has the smallest EtOH concentration provides an estimate of the eutectic point. The ratio $w_{(-)}/w_{(+)}$ at the eutectic point decreases with increasing temperature and decreasing EtOH concentration, being 11.6 at 25°, 10.9 at 35°, and reaching 7.7 at 50°. The tendency of this ratio to decrease with increasing temperature and decreasing EtOH content is consistent with the aforementioned value measured for the binary system consisting of the two pure enantiomers in a ratio of *ca.* 5.7.

Table 3. *Measured Mass Fractions* $w_{(+)}$ *and* $w_{(-)}$ *in Ternary Systems* (see *Fig. 4*). Data points with 95% confidence intervals given in order of decreasing $w_{(+)}$.

T [°]	$w_{(+)}$	$w_{(-)}$	w_{EtOH}
25.0	0.0139 ± 0.0002	0.0137 ± 0.0002	0.9274
	0.0118 ± 0.0002	0.0155 ± 0.0002	0.9727
	0.0110 ± 0.0010	0.0193 ± 0.0019	0.9697
	0.0102 ± 0.0002	0.0170 ± 0.0006	0.9728
	0.0057 ± 0.0006	0.0377 ± 0.0034	0.9566
	0.0052 ± 0.0001	0.0406 ± 0.0006	0.9542
Eutectic →	0.0043 ± 0.0002	0.0500 ± 0.0005	0.9457
	0.0023 ± 0.0001	0.0508 ± 0.0007	0.9469
	0.0000	0.0518 ± 0.0001	0.9482
35.0	0.0204 ± 0.0011	0.0202 ± 0.0012	0.9594
	0.0167 ± 0.0004	0.0281 ± 0.0007	0.9552
	0.0122 ± 0.0007	0.0344 ± 0.0019	0.9534
	0.0110 ± 0.0003	0.0392 ± 0.0010	0.9498
	0.0096 ± 0.0001	0.0570 ± 0.0007	0.9334
Eutectic →	0.0068 ± 0.0001	0.0738 ± 0.0006	0.9194
	0.0043 ± 0.0001	0.0750 ± 0.0009	0.9207
	0.0000	0.0790 ± 0.0010	0.9210
50.0	0.0360 ± 0.0004	0.0358 ± 0.0003	0.9282
	0.0180 ± 0.0012	0.0772 ± 0.0053	0.9048
Eutectic →	0.0167 ± 0.0011	0.1287 ± 0.0022	0.8546
	0.0122 ± 0.0007	0.1297 ± 0.0080	0.8581
	0.0000	0.1185 ± 0.0008	0.8815

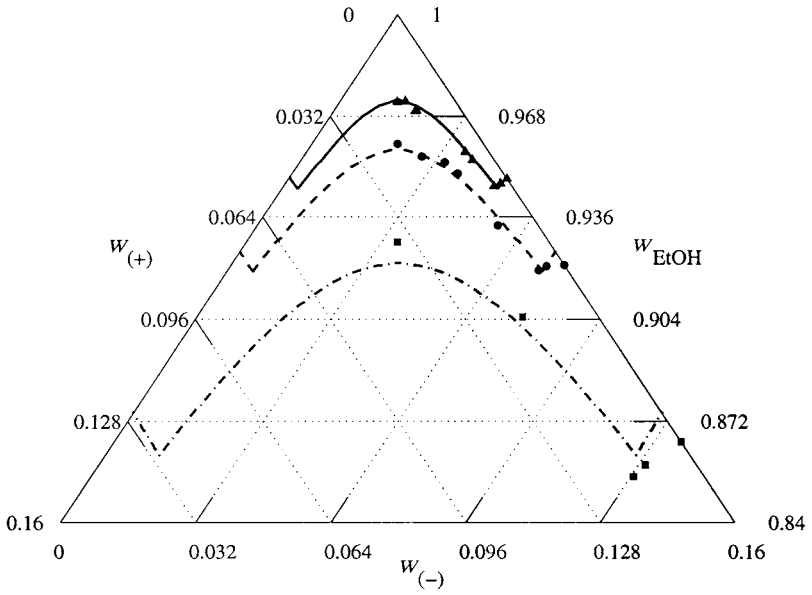

Fig. 4. *Ternary solubility diagram of* Tröger's *base enantiomers in EtOH*. Experimental data points and calculated curves: 25° (triangles, solid line), 35° (circles, dashed line), and 50° (squares, dashed-dotted line).

It is worth pointing out that the solutions with a $w_{(+)}$ value larger than that corresponding to the eutectic point are at equilibrium with the solid racemic compound, whereas those with a $w_{(+)}$ value smaller than the eutectic value are at equilibrium with crystals of the pure (−)-enantiomer (see also *Fig. 1*, *b*). Obviously, the eutectic solution is at equilibrium both with crystals of the pure (−)-enantiomer and of the racemic compound, as has been confirmed by independently analyzing the composition of dried crystals harvested at equilibrium conditions.

3.3. *Solid-Phase Properties.* In this section, we analyze the properties of the enantiopure crystals and of the crystals of the racemic compound. Under the microscope (see *Fig. 5*), the two types of crystals exhibit different habits and shapes; in fact, the racemic compound crystallizes from EtOH as fine needles, whereas the enantiopure crystals form coarse, bulky crystals with an aspect ratio close to 1.

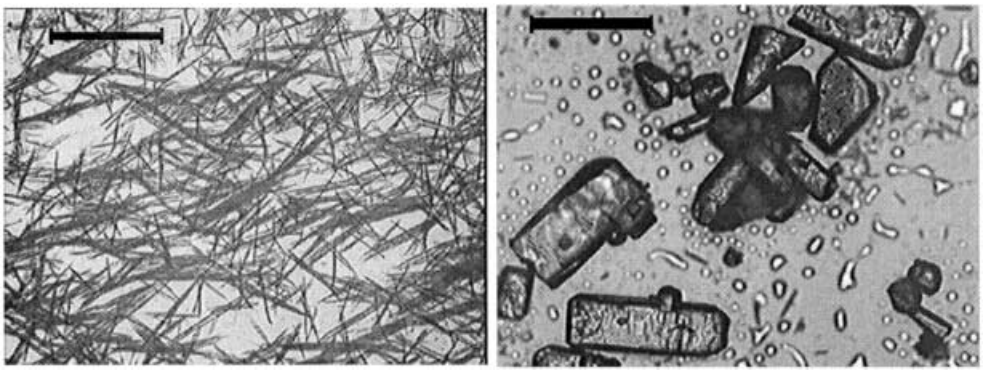

Fig. 5. *Photomicrographs of crystals of racemic (±)-*Tröger*'s base* (left) *and (−)-*Tröger*'s base* (right) *precipitated from EtOH*. The reference bar corresponds to 50 μm.

First, TGA was performed to clarify whether these solid phases occur as solvates or as pure crystals. Samples of enantiopure or racemic crystals were transferred directly from the equilibration flasks to the TGA cells after simple membrane filtration. The recorded mass profiles obtained under linear heating from 30° to 120° over 5400 s are shown for the two types of crystals in *Fig. 6*. The mass of enantiopure crystals remains constant, while, on the other hand, the mass of racemic crystals decreases during the first 2000 s, *i.e.*, between 30° and 65°, and then stays at a constant value. It is worth noting that such behavior has been confirmed by repeating these measurements at various heating rates and also at constant temperature; in all cases, no kinks in the mass-loss curve of the racemic crystals, which might indicate the presence of solvent bound in different ways to the crystals, were observed. These results indicate that both types of crystals precipitate as pure *Tröger*'s base, *i.e.*, no solvates are formed. However, the amount of residual solvent present on the crystals after filtration is significantly different for the enantiopure than for the racemic crystals, possibly due to their significantly different shapes. In other words, drying is much faster for the enantiopure than for the racemic crystals, hence, in the former case, it takes place already on the filter or during the start-up of the TGA experiment.

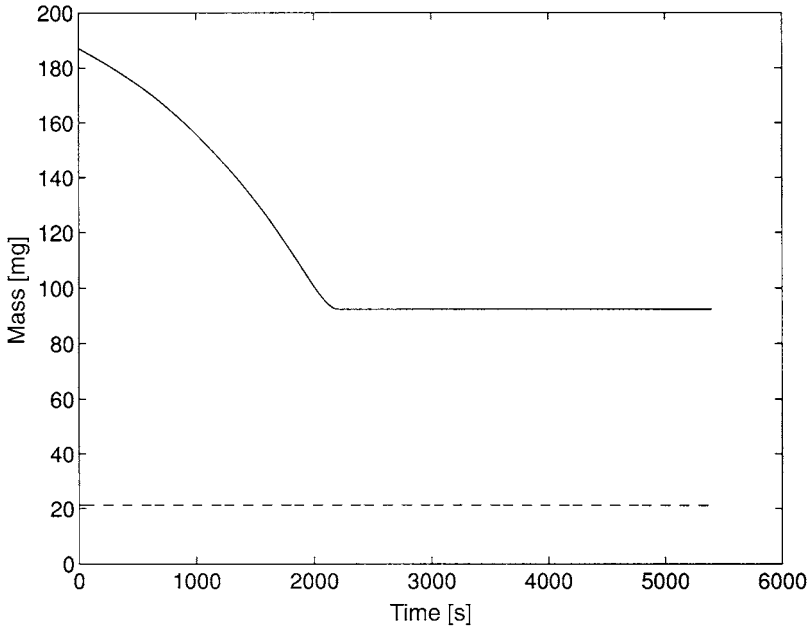

Fig. 6. *TGA Measurement for crystals of (−)-*Tröger*'s base* (dashed line) *and of racemic compound* (solid line) *precipitated from EtOH*. Temperature profile: linear heating from 30° – 120° in 90 min.

Next, XRD analysis of the precipitated racemic and enantiopure crystals was carried out. The crystal morphology of the racemic compound was found to correspond to that of the orthorhombic structure (space group *Pccn*, with $Z = 12$) reported previously [20]. The crystal structure of the pure enantiomer, which has not been reported in the literature before, was determined to be orthorhombic as well. An illustration of the molecular packing of (+)-*Tröger*'s base as analyzed from XRD data is given in *Fig. 7*. The X-ray crystal data of (+)-*Tröger*'s base at 293 K are as follows: orthorhombic, space group $P2_12_12_1$ (no. 19), $D = 1.211$ g cm^{-3}, $Z = 4$, $a = 6.110(6)$, $b = 7.934(7)$, $c = 28.33(6)$ Å, $V = 1373(3)$ Å^3. *Picker–Stoe* diffractometer, CuK_α radiation, $\lambda = 1.5418$ Å. The structure was solved by direct methods and refined by full-matrix least-squares analysis (SHELXTL PLUS). All heavy atoms were refined anisotropically, H-atoms fixed isotropically with atomic positions based on stereochemical considerations. Final $R(F) = 0.055$, $wR(F^2) = 0.136$ for 174 parameters and 626 reflections with $I > 2\sigma(I)$ and $3.54° < \Theta < 50.0°$ (corresponding *R*-values based on all 859 reflections are 0.077 and 0.156, respectively). *Cambridge Crystallographic Data Centre* deposition No. CCDC 211453. Copies of the crystallographic data can be obtained, free of charge, on application to *CCDC*, 12 Union Road, Cambridge CB2 1EZ, UK (fax: (+44) 1223-336-033; e-mail: deposit@ccdc.cam.ac.uk).

4. Modelling of the Solid-Liquid Equilibrium. – In this section, the basic model equations that describe solid-liquid equilibria and, in particular, that describe the equilibria for a system including enantiomers are presented. Due to the formation of a

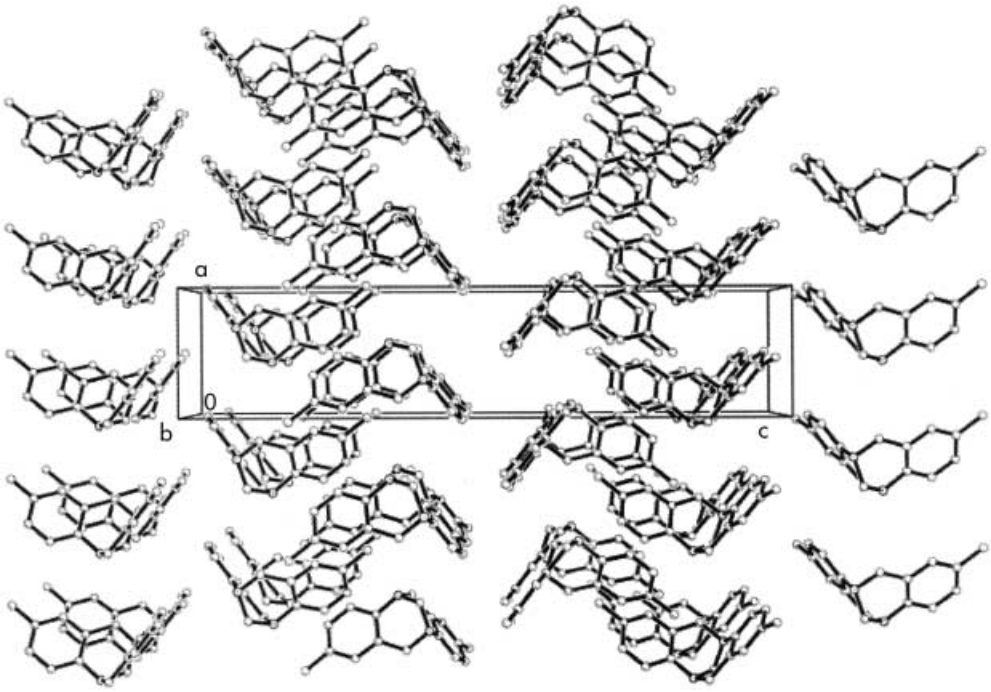

Fig. 7. *Molecular packing diagram of the (+)-*Tröger*'s base enantiomer*

racemic compound, the description of the solid-liquid equilibrium of the system includes two different equilibrium situations (see *Fig. 1,a*), namely equilibrium either with solid racemic crystals or with solid enantiopure crystals. For the sake of simplicity, the components, the (+)- and (−)-enantiomers of *Tröger*'s base and the solvent EtOH are indicated by the subscripts 1, 2, and 3, respectively, in the notation of the following sections. The solid racemic compound is labelled with subscript r.

For the equilibrium condition at temperature T between pure crystals of one enantiomer and a liquid phase constituted of the same enantiomer and of either the other enantiomer or the solvent or both, the *Schröder–van Laar* equation (*Eqn. 1*) must be fulfilled under rather standard thermodynamic assumptions [3][21][22]:

$$\ln x_i\gamma_i = \frac{\Delta_{\text{fus}}H_i(T_{\text{m},i})}{R}\left(\frac{1}{T_{\text{m},i}} - \frac{1}{T}\right), \tag{1}$$

where $i = 1$ (or 2) corresponds to the enantiomer whose crystals are present, x_i and γ_i are the mole fraction and activity coefficient, respectively, in solution, $T_{\text{m},i}$ and $\Delta_{\text{fus}}H_i$ are the melting temperature and enthalpy (per unit mole) of the same enantiomer.

In the second case, *i.e.*, at equilibrium between a binary or a ternary solution (including the solvent) and the racemic solid compound, the *Vieland* equation (*Eqn. 2*) is valid under the same assumptions as before [3][22][23]:

$$\ln(4x_1\gamma_1x_2\gamma_2) = \frac{\Delta_{fus}H_r(T_{m,r})}{RT}\left(\frac{1}{T_{m,r}} - \frac{1}{T}\right), \tag{2}$$

where $T_{m,r}$ and $\Delta_{fus}H_r$ are the melting temperature and enthalpy of the racemic solid compound. Note that $\Delta_{fus}H_r$ refers to one mole of one enantiomer in the racemic compound. *Eqn. 2* is valid for both binary and ternary systems. In a binary system, the molar fractions x_i and x_j of the components i and j are related by

$$x_j = 1 - x_i, \tag{3}$$

with $i, j = 1, 2$, and $i \neq j$, while

$$x_j = 1 - x_i - x_3 \tag{4}$$

with $i, j = 1, 2$, and $i \neq j$, is valid in the case of a ternary system.

In this study, the non-random two-liquids (NRTL) approach is applied to describe activity coefficients γ_i for binary and ternary systems involving (+)- and (−)-*Tröger*'s base and EtOH [21][24][25].

Neglecting third- and higher-order interactions terms in the NRTL description, the activity coefficient, γ_i, in a system with m components are given by [21]:

$$\ln\gamma_i = \frac{\sum_{i=1}^{m}\tau_{ji}G_{ji}x_j}{\sum_{l=1}^{m}G_{li}x_l} + \sum_{j=1}^{m}\frac{x_jG_{ij}}{\sum_{l=1}^{m}G_{lj}x_l}\left(\tau_{ij} - \frac{\sum_{r=1}^{m}x_r\tau_{rj}G_{rj}}{\sum_{l=1}^{m}G_{lj}x_l}\right) \tag{5}$$

with $\tau_{ii} = 0$ and $G_{ii} = 1$. Temperature dependence is described by the parameters G_{ji}, which are defined as:

$$G_{ji} = \exp(-\alpha_{ji}\tau_{ji}), \tag{6}$$

where $\alpha_{ji} = \alpha_{ij}$, and it is related to the non-randomness of the mixture, and

$$\tau_{ji} = \frac{g_{ji} - g_{ii}}{RT}, \tag{7}$$

with g_{ji} being an energy parameter characteristic of the *i-j* interaction and the difference $\Delta g_{ji} = g_{ji} - g_{ii}$ is assumed to be temperature independent.

In the special case of a ternary system ($m = 3$) that includes two enantiomers and a solvent, the following simplifications can be applied due to symmetry. The nonidealities between solvent ($i = 3$) and each enantiomer ($i = 1$ or 2) are identical, *i.e.:*

$$\tau_{13} = \tau_{23}, \tag{8}$$

$$\tau_{31} = \tau_{32}, \tag{9}$$

$$\alpha_{13} = \alpha_{23} = \alpha_{31} = \alpha_{32} = \alpha, \tag{10}$$

thus leading to

$$G_{13} = G_{23} \tag{11}$$

$$G_{31} = G_{32}. \tag{12}$$

Moreover, we also assume that the two enantiomers behave as an ideal binary system in the liquid phase, both with and without the solvent. This requires that:

$$\tau_{12} = \tau_{21} = 0 \tag{13}$$

$$G_{12} = G_{21} = 1. \tag{14}$$

In summary, the following three independent parameters must be assigned to characterize the behavior of solutions of the two enantiomers and the solvent: α, $\Delta g_{13} = \Delta g_{23}$, and $\Delta g_{31} = \Delta g_{32}$. The estimation of the NRTL parameters is based on minimization of the least-squares objective functions using a *Nelder–Mead* simplex (direct search) minimization routine [26].

5. Modelling Results and Discussion. – In this section, the model approach described in *Section 4* is applied to describe the experimental results presented in *Section 3*. Two alternative descriptions of the liquid phase are considered, *i.e.*, as an ideal phase where $\gamma_i = 1$, or as a nonideal mixture with $\gamma_i \neq 1$, as described by the NRTL model. The former approach effectively describes the solid-liquid equilibrium of the *Tröger*'s base enantiomers, as illustrated in *Fig. 3*, where the symbols are the experimental points and the curves are the calculated *liquidus* line (solid curve) and *solidus* line (dashed curve) based on *Eqns. 1* and *2*, on the left and the right hand sides of the eutectic, respectively. The parameters in the equations are those obtained from DSC measurements, and $\gamma_i = 1$ for ideality. The model leads to a eutectic weight fraction of $w_{(+)} = 0.156$ and a eutectic temperature of 118.7°, *i.e.*, in good agreement with the experimental data (see *Fig. 2*).

Estimates of the solubility in EtOH of both the enantiopure forms and the racemic compound are seriously in error when an ideal liquid phase is assumed (see *Fig. 8*). Therefore, in the presence of EtOH in all cases, nonideal-solution behavior is to be accounted for, possibly through the NRTL model discussed above. We have estimated the three model parameters using either the solubility data of pure enantiomer and racemate reported in *Fig. 8* only (leading to $\Delta g_{13} = \Delta g_{23} = 2627$ J/mol, $\Delta g_{31} = \Delta g_{32} = 1962$ J/mol and $\alpha = -0.48$), or all the equilibrium data reported in *Fig. 4* and *Table 3* (leading to $\Delta g_{13} = \Delta g_{23} = 2654$ J/mol, $\Delta g_{31} = \Delta g_{32} = 1651$ J/mol and $\alpha = -0.55$). It is worth noting that the two parameter sets are rather similar, and that the curves obtained in the two cases for the solubility curves of *Fig. 8* and for the isothermal equilibrium curves of *Fig. 4* are indistinguishable. It can readily be observed that the agreement between calculated results and experimental data is rather satisfactory over the whole range of composition and temperature spanned in *Fig. 4*. Hence, the model allows us to predict the solubility of *Tröger*'s base enantiomers in EtOH in the investigated temperature range.

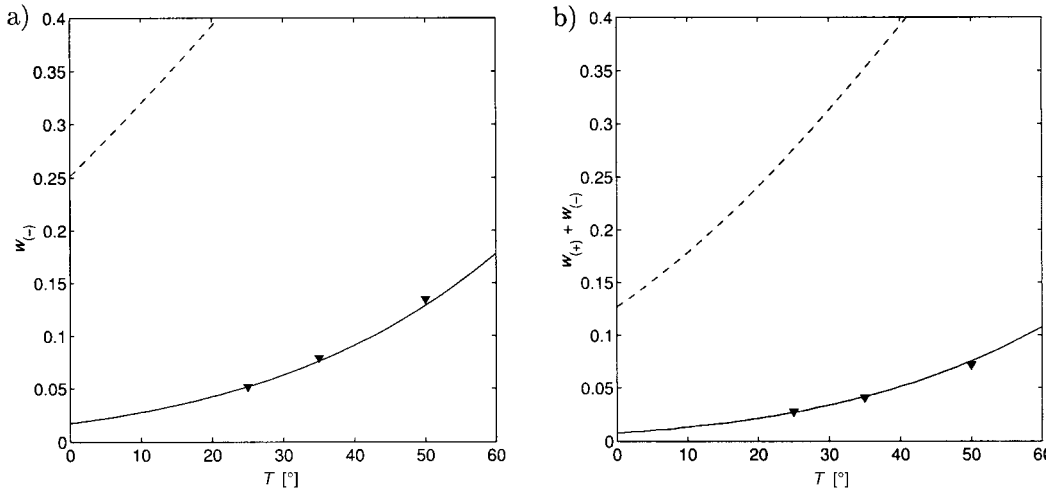

Fig. 8. *Solubility of* Tröger*'s base in EtOH as a function of temperature.* Experimental data (triangles); ideal equilibrium (dashed line); nonideal equilibrium as described in the text (solid line). *a*) Pure (−)-*Tröger*'s base solubility in units of mass fraction $w_{(-)}$. *b*) (±)-*Tröger*'s base racemate $w_{(+)} = w_{(-)}$ solubility in units of mass fraction $w_{(+)} + w_{(-)}$.

In summary, the results suggest a rather systematic procedure to obtain ternary solid-liquid phase equilibria for enantiomeric systems. First, DSC measurements are used to analyze the general characteristics of the binary (+)/(−)-enantiomer system, including the type of the binary equilibrium, melting temperatures, and melting enthalpies. In a second step, solubility data of pure enantiomers and of the racemic mixture in the solvent are measured. Here, no chiral separation is needed for the experimental analysis. In the case of the system investigated in this work, namely that of *Tröger*'s base in EtOH, the use of solubility data combined with the data of melting temperature and melting enthalpy of pure enantiomer and racemate allowed for a rather accurate description of the ternary diagram by application of the NRTL model to account for solution nonideality. This model can then be used to predict solid-liquid equilibria across the whole temperature range investigated, or to get guidelines for further measurements, *e.g.*, to more accurately locate eutectic points by means of ternary measurements.

The authors wish to thank Mr. *Roger Müller* of the Institute of Process Engineering of ETH Zurich for his help in carrying out the TGA measurements.

REFERENCES

[1] J. E. Rekoske, *AIChE J.* **2001**, *47*, 2.
[2] E. Francotte, J. Richert, *J. Chromatogr. A* **1997**, *769*, 101.
[3] J. Jacques, A. Collet, 'Enantiomers, Racemates, and Resolutions', Wiley & Sons, New York, 1981.
[4] A. Collet, *Enantiomer* **1999**, *4*, 157.
[5] K. Mihlbachler, K. Kaczmarski, A. Seidel-Morgenstern, G. Guiochon, *J. Chromatogr. A* **2002**, *955*, 35.
[6] S. Beilles, P. Cardinael, E. Ndzie, S. Petit, G. Coquerel, *Chem. Eng. Sci.* **2001**, *56*, 2281.
[7] B. G. Lim, C. B. Ching, R. B. H. Tan, S. C. Ng, *Chem. Eng. Sci.* **1995**, *50*, 2289.

[8] M. Juza, M. Mazzotti, M. Morbidelli, *Trends Biotechnol*. **2000**, *18*, 108.
[9] H. Lorenz, P. Sheehan, A. Seidel-Morgenstern, *J. Chromatogr. A* **2001**, *908*, 201.
[10] J. Jacques, J. Gabard, *Bull. Soc. Chim. Fr*. **1972**, 342.
[11] B. G. Lim, R. B. H. Tan, S. C. Ng, C. B. Ching, *Chirality* **1995**, *7*, 74.
[12] H. Lorenz, A. Seidel-Morgenstern, *Thermochim. Acta* **2002**, *382*, 129.
[13] X. Wang, X. J. Wang, C. B. Ching, *Chirality* **2002**, *14*, 318.
[14] M. P. Pedeferri, G. Zenoni, M. Mazzotti, M. Morbidelli, *Chem. Eng. Sci*. **1999**, *54*, 3735.
[15] A. Seidel-Morgenstern, G. Guiochon, *Chem. Eng. Sci*. **1993**, *48*, 2787.
[16] A. Seidel-Morgenstern, S. C. Jacobson, G. Guiochon, *J. Chromatogr. A* **1993**, *637*, 19.
[17] C. Migliorini, M. Mazzotti, G. Zenoni, M. Pedeferri, M. Morbidelli, *AIChE J*. **2000**, *46*, 1530.
[18] B. G. Bag, *Curr. Sci*. **1995**, *68*, 279.
[19] B. Baldeyrou, C. Tardy, C. Bailly, P. Colson, C. Houssier, F. Charmantray, M. Demeunynck, *Eur. J. Med. Chem*. **2002**, *37*, 315.
[20] S. B. Larson, C. S. Wilcox, *Acta Crystallogr., Sect. C* **1986**, *42*, 224.
[21] J. M. Prausnitz, R. N. Lichtenthaler, E. G. de Azevedo, 'Molecular Thermodynamics of Fluid-Phase Equilibria', Prentice Hall PTR, Upper Saddle River, NJ, 1999.
[22] M. Radomska, R. Radomski, *Thermochim. Acta* **1980**, *40*, 405.
[23] I. Prigogine, R. Defay, 'Chemical Thermodynamics', Longman, London, UK, 1973.
[24] S. Bruin, J. M. Prausnitz, *Ind. Eng. Chem. Proc. Design Dev*. **1971**, *10*, 562.
[25] B. Eck, 'Thermodynamisch konsistente Beschreibung des Feststoff-Flüssigkeits-Phasengleichgewichts zweier technisch bedeutender Stoffsysteme mit Komplexbildung', Shaker Verlag, Aachen, 2000.
[26] J. A. Nelder, R. Mead, *Comput. J*. **1965**, *7*, 308.

Received July 2, 2003